2013 European Control Conference (ECC)
July 17-19, 2013, Zürich, Switzerland.

Contribution plots for Statistical Process Control: analysis of the smearing-out effect

Pieter Van den Kerkhof[1], Jef Vanlaer[1], Geert Gins[1], and Jan F.M. Van Impe[1,2]

***Abstract*— Since the generation of contribution plots requires no a priori information about the detected disturbance (e.g., historical faulty data), it is a popular fault isolation technique in Statistical Process Control (SPC). However, Westerhuis *et al.* reported that contribution plots suffer from fault smearing, i.e., the influence of faulty variables on the contributions of non-faulty variables, which complicates the fault isolation task as variables unaffected by the fault may be highlighted and faulty variables obscured [1]. This paper presents an analysis of the smearing effect for three general contribution computation methods: Complete Decomposition, Partial Decomposition and Reconstruction-Based contributions. The analysis shows that (*i*) smearing is present in all three methods, (*ii*) smearing depends on the chosen number of principal components of the underlying latent variable model and (*iii*) the extent of smearing increases for variables correlated in the training data for a well-chosen model order. The effect of smearing on the isolation performance of single and multiple sensor faults of various magnitudes is illustrated using a simulation case study. The results indicate that correct isolation with contribution plots is not guaranteed for multiple sensor faults. Furthermore, contribution plots only outperform univariate fault isolation for single sensor faults with small magnitudes. For multiple sensor faults, univariate fault isolation exhibits a significantly larger correct fault isolation rate. Based on the smearing analysis and the results for sensor faults, the authors advise to use contributions only if a sound physical interpretation of the principal components is available.**

I. Introduction

Abnormal event management is of central importance to the process industries. Early detection and diagnosis of process faults permits timely interventions to keep the process within a safe controllable operating region and avoids production loss associated with the abnormal situation. Statistical Process Control (SPC) is a set of data-based techniques for process monitoring, fault detection and fault diagnosis. Due to the abundance of sensors in today's process plants, extensive historical databases containing frequent measurements of online sensors on hundreds of variables are becoming a commodity for process engineers. Therefore, employing SPC to exploit these existing databases has tremendous potential and has already resulted in a large number of industrial applications.

The basic concept of SPC is the statistical comparison of the current process measurements with historical data obtained under Normal Operating Conditions (NOC). Process behavior not included in the NOC data is detected by fault detection statistics. The process is monitored using control charts which depict the value of the statistic and corresponding control limits for normal operation at each time point.

Statistical projection methods such as Principal Component Analysis (PCA [2]) and Partial Least Squares (PLS [3]) greatly simplify fault detection by reducing the multivariate and typically heavily correlated sensor data to a smaller set of uncorrelated latent variables. The successful application of PCA and PLS has been reported extensively in literature and has become a standard approach to SPC since its introduction in the early nineties [4], [5].

Upon detection of a process disturbance, the multivariate control charts do not provide any information about the root cause of the abnormal situation. If a sufficient amount of historical data of all of the process faults is available, classification methods can achieve conclusive diagnosis results by assigning the fault to the class the new measured data most resembles. However, as the process is designed and controlled to remain in the normal operating region, the availability of such data is often a bottleneck for developing an adequate classifier.

Alternatively, the underlying PCA or PLS model can be investigated by examining contribution plots, which chart the contribution of each variable to the out-of-control statistic [6]. Because of its ease of implementation and the absence of a need for historical faulty data, contribution plots are by far the most popular approach to find the cause of an alarm signal in SPC and have found extensive use in applications (see e.g., [7], [8], [9], [10]). Westerhuis *et al.* were the first to report the propagation of contributions of faulty variables to the contributions of variables not influenced by the fault [1]. This 'smearing-out' effect quickly leads to ambiguous diagnosis results for complex process faults. Different contribution computation methods were proposed in the literature. Alcala and Qin showed that each of them is affected by smearing [11]. Hence, a profound understanding of the smearing effect is imperative for the choice of a contribution computation technique and a correct interpretation of the fault isolation results.

The goal of this paper is to provide a deeper insight into

[1]Chemical and Biochemical Process Technology and Control (BioTeC), Department of Chemical Engineering, Katholieke Universiteit Leuven, W. De Croylaan 45, B-3001 Heverlee (Belgium) Email: {pieter.vandenkerkhof, jef.vanlaer, geert.gins, jan.vanimpe}@cit.kuleuven.be

[2]Corresponding author

*Work supported in part by Project PVF/10/002 (OPTEC Optimization in Engineering Center) of the Research Council of the KU Leuven, Project KP/09/005 (SCORES4CHEM) of the Industrial Research Council of the KU Leuven, and the Belgian Program on Interuniversity Poles of Attraction initiated by the Belgian Federal Science Policy Office. P. Van den Kerkhof and J. Vanlaer are funded by a Ph.D grant of the agency for Innovation by Science and Technology (IWT). J. Van Impe holds the chair Safety Engineering sponsored by the Belgian chemistry and life sciences federation essenscia. The authors assume scientific responsibility.

978-3-952-41734-8/©2013 EUCA

the smearing effect for contribution plots. The remainder of this paper is structured as follows. Section II contains a concise description of contribution computation. Section III presents an analysis of the causes of contribution smearing for three popular general types of contribution computation methods. In Section IV the influence of smearing on fault isolation is further studied for the case of sensor faults and referenced against isolation based directly on the pretreated data. Section V ties the analysis and case study results together to draw some conclusions.

II. Contribution plots

Contribution plots rely on the investigation of the underlying statistical projection method. This paper focuses on basic PCA for ease of explanation and because of its popularity in industrial applications. The derived formulas can be readily extended to other statistical projection methods (see, e.g., Westerhuis *et al.* [1]). Section II-A briefly describes the basics of PCA based process monitoring and Section II-B discusses the theory of contribution computation.

A. PCA based monitoring

Consider an industrial data set consisting of m measurements on n variables organized in an $m \times n$ data matrix $\mathbf{X}$. Before applying PCA, each column of $\mathbf{X}$ is scaled to zero mean and unit variance (i.e., auto-scaling). For the remainder of this paper, the data is assumed to be auto-scaled. PCA divides the original $\mathcal{R}^n$ measurement space into a model space spanned by principal components (the model hyperplane) and a residual space [2]. The principal components are obtained from the eigen-decomposition of the covariance matrix $\mathbf{S}$ of $\mathbf{X}$

$$\mathbf{S} = \frac{1}{m-1}\mathbf{X}^{\mathrm{T}}\mathbf{X} \tag{1}$$

$$= \begin{bmatrix}\mathbf{P} & \tilde{\mathbf{P}}\end{bmatrix}\begin{bmatrix}\mathbf{\Lambda} & \mathbf{0} \\ \mathbf{0} & \tilde{\mathbf{\Lambda}}\end{bmatrix}\begin{bmatrix}\mathbf{P} & \tilde{\mathbf{P}}\end{bmatrix}^{\mathrm{T}} \tag{2}$$

where $\mathbf{P} \in \mathcal{R}^{n\times r}$ contains the r eigenvectors of $\mathbf{S}$ associated with the r largest eigenvalues contained in a diagonal matrix $\mathbf{\Lambda} \in \mathcal{R}^{r\times r}$ and $\tilde{\mathbf{P}} \in \mathcal{R}^{n\times n-r}$ holds the eigenvectors corresponding to the remaining eigenvalues contained in a diagonal matrix $\tilde{\mathbf{\Lambda}} \in \mathcal{R}^{n-r\times n-r}$. The number of retained principal components r is decided by the user. The columns of $\mathbf{P}$ and $\tilde{\mathbf{P}}$ span the model hyperplane and residual space respectively. A measurement vector $\mathbf{x} \in \mathcal{R}^n$ can therefore be decomposed into two vectors

$$\hat{\mathbf{x}} = \mathbf{P}\mathbf{P}^{\mathrm{T}}\mathbf{x} \tag{3}$$

$$\tilde{\mathbf{x}} = \tilde{\mathbf{P}}\tilde{\mathbf{P}}^{\mathrm{T}}\mathbf{x} \tag{4}$$

with $\hat{\mathbf{x}}$ and $\tilde{\mathbf{x}}$ the projections of $\mathbf{x}$ on the model and residual spaces, respectively. $\mathbf{x}$ can be represented in a new coordinate system defined by the columns of $\mathbf{P}$

$$\mathbf{t} = \mathbf{x}^{\mathrm{T}}\mathbf{P} \tag{5}$$

where $\mathbf{t} \in \mathcal{R}^{r\times 1}$ contains the so-called scores of $\mathbf{x}$ that represent $\mathbf{x}$ by a reduced set of r uncorrelated variables.

The measurement vector $\mathbf{x}$ is subjected to fault detection by computing fault detection indices. The general formula for quadratic fault detection indices is

$$\text{Index}\,(\mathbf{x}) = \|\mathbf{x}\|^2_{\mathbf{M}} = \mathbf{x}^{\mathrm{T}}\mathbf{M}\mathbf{x} \tag{6}$$

where $\mathbf{M}$ depends on the specific fault detection statistic. For the popular Squared Prediction Error (SPE) and Hotelling's T^2 statistics, $\mathbf{M}$ is equal to

$$\mathbf{M}_{\text{SPE}} = \tilde{\mathbf{P}}\tilde{\mathbf{P}}^{\mathrm{T}}, \tag{7}$$

$$\mathbf{M}_{\mathrm{T}^2} = \mathbf{P}\mathbf{\Lambda}^{-1}\mathbf{P}^{\mathrm{T}}. \tag{8}$$

The matrices $\mathbf{M}_{\text{SPE}}$ and $\mathbf{M}_{\mathrm{T}^2}$ are symmetric and positive (semi-)definite. $\mathbf{M}_{\text{SPE}}$ is also idempotent.

B. Contribution computation

The use of contribution plots for Statistical Process Control (SPC) was introduced by MacGregor *et al.* in order to investigate the underlying PCA or PLS model when a fault detection statistic exceeds its control limit [12], [13]. MacGregor *et al.* decompose the fault detection statistic into a sum of terms, each associated with one variable, called contributions. The assumption behind contribution computation is that variables associated with the fault exhibit large contributions. In this case, a contribution plot enables engineers and operators to focus their attention on a small subset of variables and therefore facilitates the diagnostic task.

As there is no unique way to decompose a fault detection statistic into a sum of terms each assigned to a single variable, various authors proposed different formulas for contribution computation. Alcala and Qin unified these into three general methods: complete decomposition, partial decomposition and reconstruction-based contributions [14].

1) Complete Decomposition (CD): The CD contribution of the i-th variable is defined by Alcala and Qin as

$$\text{CD}_i = \left(\xi_i^{\mathrm{T}}\mathbf{M}^{\frac{1}{2}}\mathbf{x}\right)^2 \tag{9}$$

where ξ_i is the i-th column of the $n\times n$ identity matrix [14]. CD contributions are always positive and their sum is equal to the value of the corresponding statistic.

2) Partial Decomposition (PD): Alcala and Qin [14] define the PD contribution of the i-th variable as

$$\text{PD}_i = \mathbf{x}^{\mathrm{T}}\mathbf{M}\xi_i\xi_i^{\mathrm{T}}\mathbf{x}. \tag{10}$$

As for CD contributions, the sum of the PD contributions equals the value of the corresponding fault detection statistic. However, PD contributions can attain negative values. When a variable is equal to its mean or expected value, i.e., $\xi_i^{\mathrm{T}}\mathbf{x} = x_i = 0$, its PD contribution is equal to zero.

3) Reconstruction-Based (RB): RB contributions were proposed in [11] as

$$\text{RB}_i = \frac{\left(\xi_i^{\mathrm{T}}\mathbf{M}\mathbf{x}\right)^2}{\xi_i^{\mathrm{T}}\mathbf{M}\xi_i} \tag{11}$$

RB contributions are always positive. Unlike CD and PD contributions, their sum is not guaranteed to be equal to the value of the corresponding statistic.

III. THE SMEARING EFFECT

Westerhuis *et al.* were the first to report that faulty variables influence the contribution of non-faulty variables [1]. The effect of a fault is smeared out over the different contributions and the difference between contributing and non-contributing variables decreases. This section analyzes the smearing behavior of CD, PD and RB contributions to provide a deeper understanding of the cause and nature of contribution smearing.

A. Smearing of CD contributions

Substituting $\mathbf{M}$ in Eq. 9 by $\tilde{\mathbf{P}}\tilde{\mathbf{P}}^{\mathrm{T}}$ for the SPE statistic and $\mathbf{P}\mathbf{\Lambda}^{-1}\mathbf{P}^{\mathrm{T}}$ for the T^2 statistic yields their CD contributions.

$$\mathrm{CD}_i^{\mathrm{SPE}} = \left(\xi_i^{\mathrm{T}} \left(\tilde{\mathbf{P}}\tilde{\mathbf{P}}^{\mathrm{T}}\right)^{\frac{1}{2}} \mathbf{x}\right)^2 \tag{12}$$

$$\mathrm{CD}_i^{\mathrm{T}^2} = \left(\xi_i^{\mathrm{T}} \left(\mathbf{P}\mathbf{\Lambda}^{-1}\mathbf{P}^{\mathrm{T}}\right)^{\frac{1}{2}} \mathbf{x}\right)^2 \tag{13}$$

By using the idempotent property of $\tilde{\mathbf{P}}\tilde{\mathbf{P}}^{\mathrm{T}}$ and Eq. 4, the CD contributions to the SPE statistic reduce to

$$\mathrm{CD}_i^{\mathrm{SPE}} = \left(\xi_i^{\mathrm{T}}\tilde{\mathbf{P}}\tilde{\mathbf{P}}^{\mathrm{T}}\mathbf{x}\right)^2 \tag{14}$$

$$= \left(\xi_i^{\mathrm{T}}\tilde{\mathbf{x}}\right)^2 = \tilde{x}_i^2. \tag{15}$$

The above derivation demonstrates that the CD contributions to the SPE statistic are equal to the squared components of the residual vector $\tilde{\mathbf{x}}$ along each axis of the original measurement space. The residual vector is computed by projecting the measurement vector on the residual subspace and expressing the resulting vector in the original coordinates. The compression to a smaller number of subspace variables and subsequent expansion back to the measurement space enables faulty and non-faulty variables to interact which is the fundamental cause of contribution smearing.

For the T^2 statistic, Eq. 13 can be rewritten as

$$\mathrm{CD}_i^{\mathrm{T}^2} = \left(\xi_i^{\mathrm{T}}\mathbf{P}\mathbf{\Lambda}^{-\frac{1}{2}}\mathbf{P}^{\mathrm{T}}\mathbf{x}\right)^2 \tag{16}$$

$$= \left(\xi_i^{\mathrm{T}}\mathbf{P}\mathbf{\Lambda}^{-\frac{1}{2}}\mathbf{t}^{\mathrm{T}}\right)^2. \tag{17}$$

To obtain the CD contributions to the T^2 statistic, $\mathbf{x}$ is projected onto the model plane to obtain the scores $\mathbf{t}$. Each score is scaled by its standard deviation before expressing the score vector in the original measurement space. Similar to the SPE contributions, the compression and subsequent expansion enables faulty and non-faulty variables to interact.

To gain further insight into the smearing phenomenon, it is instructive to rewrite the two contribution formulas (Eqs. 12, 13) in a different form. At the mathematical core of each contribution formula is a simple linear combination of the measured variables. The CD contributions to the SPE and T^2 statistic can be rewritten as

$$\mathrm{CD}_i^{\mathrm{SPE}} = \left(\alpha_i x_i + \sum_{j=1, j\neq i}^{n} \gamma_{ij} x_j\right)^2 \tag{18}$$

$$\mathrm{CD}_i^{\mathrm{T}^2} = \left(\beta_i x_i + \sum_{j=1, j\neq i}^{n} \delta_{ij} x_j\right)^2 \tag{19}$$

where

$$\alpha_i = 1 - \sum_{l=1}^{r} p_{il}^2 \qquad \beta_i = \sum_{l=1}^{r} \lambda_l^{-\frac{1}{2}} p_{il}^2 \tag{20}$$

$$\gamma_{ij} = -\sum_{l=1}^{r} p_{il}p_{jl} \qquad \delta_{ij} = \sum_{l=1}^{r} \lambda_l^{-\frac{1}{2}} p_{il}p_{jl} \tag{21}$$

and p_{il} refers to the element at row i and column l of $\mathbf{P}$ i.e., the loading of x_i in the l-th principal component.

Three main conclusions can be drawn from the above equations. Firstly, the linear combination of all variables at the core of these equations evidences the presence of smearing. Since it is not known a priori which variables are faulty, smearing of contributing to non-contributing variables is unavoidable. Secondly, as the coefficients γ_{ij} and δ_{ij} depend on the retained number of principal components r, the contribution pattern depends on the selected model order of the PCA model. Various methods for model order selection exist and their influence on contribution plot based fault isolation is rarely, if ever, considered. Finally, since correlated variables have similar loadings in the different principal components, the extent of smearing between variables tends to increase, provided the model order r is well-chosen to adequately reflect the NOC covariance matrix. Hence, while a data plot at the moment of detection will only show increased values for variables directly influenced by the detected fault, contribution plots will also show increased values for those variables correlated with the latter variables. In the specific case of CD contributions, the influence of variable x_j on the contribution of x_i is equal to the influence of x_i on the contribution of x_j, which is clear from the expressions of γ_{ij} and δ_{ij} since $\gamma_{ij} = \gamma_{ji}$ and $\delta_{ij} = \delta_{ji}$.

B. Smearing of PD contributions

The PD contributions can be obtained by substituting $\mathbf{M}$ in Eq. 10 with $\tilde{\mathbf{P}}\tilde{\mathbf{P}}^{\mathrm{T}}$ for the SPE statistic and $\mathbf{P}\mathbf{\Lambda}^{-1}\mathbf{P}^{\mathrm{T}}$ for the T^2 statistic, yielding

$$\mathrm{PD}_i^{\mathrm{SPE}} = \mathbf{x}^{\mathrm{T}}\tilde{\mathbf{P}}\tilde{\mathbf{P}}^{\mathrm{T}}\xi_i\xi_i^{\mathrm{T}}\mathbf{x} \tag{22}$$

$$\mathrm{PD}_i^{\mathrm{T}^2} = \mathbf{x}^{\mathrm{T}}\mathbf{P}\mathbf{\Lambda}^{-1}\mathbf{P}^{\mathrm{T}}\xi_i\xi_i^{\mathrm{T}}\mathbf{x}. \tag{23}$$

The expression for the SPE statistics contributions (Eq. 22) can be rearranged by substituting Eq. 4 to obtain

$$\mathrm{PD}_i^{\mathrm{SPE}} = \tilde{\mathbf{x}}^{\mathrm{T}}\xi_i\xi_i^{\mathrm{T}}\mathbf{x} \tag{24}$$

$$= \tilde{x}_i x_i. \tag{25}$$

A variable's PD contribution to the SPE statistic equals the product of its auto-scaled value x_i and corresponding residual $\tilde{x}_i$. Hence, the cause of contribution smearing is identical to CD contributions, though the smearing effect is mitigated by multiplication with the auto-scaled variable.

Reworking the expression for the T^2 statistic (Eq. 23) using Eq. 5

$$\text{PD}_i^{\text{T}^2} = \mathbf{t}\mathbf{\Lambda}^{-1}\mathbf{P}^{\text{T}}\xi_i\xi_i^{\text{T}}\mathbf{x} \tag{26}$$
$$= \left(\xi_i^{\text{T}}\mathbf{P}\mathbf{\Lambda}^{-1}\mathbf{t}^{\text{T}}\right) x_i \tag{27}$$

results in the product of the mean centered variable x_i and a term similar to the square root of the T^2's CD contribution (Eq. 17). Although each score is scaled by its variance instead of its standard deviation, the same conclusions about smearing as in the CD case apply.

The formulas for the PD contributions can be rearranged as the product of the variable with a linear combination of all variables.

$$\text{PD}_i^{\text{SPE}} = x_i \left(\alpha_i x_i + \sum_{j=1, j\neq i}^{n} \gamma_{ij} x_j\right) \tag{28}$$

$$\text{PD}_i^{\text{T}^2} = x_i \left(\epsilon_i x_i + \sum_{j=1, j\neq i}^{n} \zeta_{ij} x_j\right) \tag{29}$$

where

$$\epsilon_i = \sum_{l=1}^{r} \lambda_l^{-1} p_{il}^2 \qquad \zeta_{ij} = \sum_{l=1}^{r} \lambda_l^{-1} p_{il} p_{jl} \tag{30}$$

The above equations lead to the same three conclusions as for the CD contributions. However, the premultiplication of x_i mitigates the smearing effect at the cost of the occurrence of counterintuitive negative contributions.

C. Smearing of RB contributions

The concept of RB contributions is to reconstruct each variable based on the other variables. When reconstructing a non-faulty variable, some of the remaining variables are faulty and faulty information is used for reconstruction. Hence, smearing is present in RB contributions by definition.

Similar arithmetics as in the CD and PD cases lead to the following expressions for RB contributions

$$\text{RB}_i^{\text{SPE}} = \left(\alpha_i x_i + \sum_{j=1, j\neq i}^{n} \gamma_{ij} x_j\right)^2 / \alpha_i \tag{31}$$

$$\text{RB}_i^{\text{T}^2} = \left(\epsilon_i x_i + \sum_{j=1, j\neq i}^{n} \zeta_{ij} x_j\right)^2 / \epsilon_i. \tag{32}$$

The above expressions are very similar to the expressions for CD contributions (Eqs. 18 and 19) and the same conclusions about the presence of smearing, the effect of r and the influence of NOC correlations are drawn. Note that, unlike CD contributions, the influence of variable x_j on the contribution of x_i is not necessarily equal to the influence of x_i on the contribution of x_j since $\gamma_{ij}/\sqrt{\alpha_i} \neq \gamma_{ji}/\sqrt{\alpha_j}$.

IV. A CASE STUDY: SENSOR FAULTS

Sensor faults are, from a fault isolation point of view, the simplest faults that can happen in a process and therefore form a useful case study to investigate the effect of contribution smearing.

A. Theoretical results

Alcala and Qin studied sensor faults where the fault-free measurements are zero, i.e., equal to their mean or expected value (for a continuous process) or lying on the average trajectory (for batch processes), and the faulty sensor has a magnitude equal to f [11]. The faulty measurement vector is of the following form

$$\mathbf{x}_f = \xi_j f. \tag{33}$$

If the contribution of the faulty variable is greater than or equal to any other fault-free variables' contribution, the fault is isolated correctly. Alcala and Qin proved for this type of single sensor faults that correct isolation is guaranteed for the PD and RB contributions but not for CD contributions [11].

In this paper, the analysis is extended to multiple sensor faults. For ease of explanation but without loss of generality, we consider two simultaneous sensor faults with a fixed magnitude f of the form

$$\mathbf{x}_{ff} = \xi_j f + \xi_k f \tag{34}$$

where $j \neq k$. From the results of Alcala and Qin, correct isolation of multiple sensor faults with CD contributions is not guaranteed [11]. It can be shown that also PD and RB contribution methods do not guarantee correct isolation of this type of faults due to the contribution smearing effect (due to space constraints the proof is omitted). Note that by the definition of $\mathbf{x}_f$ and $\mathbf{x}_{ff}$, isolation of these fault types based on the mean centered data instead of contributions is trivial since the only variables deviating from their expected value, i.e. zero, are the faulty variables.

B. Numerical illustration

The Normal Operating Conditions (NOC) data is generated according to the following process model (adapted from [14])

$$\begin{bmatrix} x_1 \\ x_2 \\ x_3 \\ x_4 \\ x_5 \\ x_6 \end{bmatrix} = \begin{bmatrix} -0.3441 & 0.4815 & 0.6637 \\ -0.2313 & -0.5936 & 0.3545 \\ -0.5060 & 0.2495 & 0.0739 \\ -0.5552 & -0.2405 & -0.1123 \\ -0.3371 & 0.3822 & -0.6115 \\ -0.3877 & -0.3868 & -0.2045 \end{bmatrix} \begin{bmatrix} t_1 \\ t_2 \\ t_3 \end{bmatrix} + \text{noise} \tag{35}$$

where t_1, t_2 and t_3 are uniformly distributed random variables with a range of $[0, 2]$, $[0, 1.6]$ and $[0, 1.2]$, respectively. The noise term consists of white Gaussian noise with zero mean and a standard deviation of 0.2. The simulated single and multiple sensor faults are of the form

$$\mathbf{x}_f = \mathbf{x}_{\text{NOC}} + \xi_j f \tag{36}$$
$$\mathbf{x}_{ff} = \mathbf{x}_{\text{NOC}} + \xi_j f + \xi_k f \tag{37}$$

where $j \neq k$, j and k are uniformly distributed among the six variables and the fault magnitude f has a range of $[0.1, 4]$. For each absolute magnitude of f, 3000 faulty samples are generated, 1500 with a negative sign and 1500 having a positive sign. 2000 NOC samples are generated for model identification. The NOC data is mean-centered and scaled to unit variance. The faulty samples are normalized similarly using the mean and variance of the NOC data. Three PCA models with respectively 2, 3 and 4 principal components are identified on the NOC data.

The computation of contributions does not require the corresponding fault detection statistic to exceed its control limit. If one statistic detects the disturbance (e.g., the SPE statistic), fault isolation can be based on the contributions to all statistics (i.e., both SPE and T^2 statistics). Therefore, the detection rate is not taken into account for assessing isolation performance and the isolation performance is examined for each generated faulty sample.

The measured correct fault isolation rates are depicted in Fig. 1. The correct isolation rates of CD (■), PD (•) and RB (▲) contributions to the SPE and T^2 statistics for single sensor faults are plotted in Figs. 1(a) and 1(c), respectively. The contributions are computed from a PCA model with 3 principal components. The dashed line represents the isolation performance achieved by using the absolute value of the (mean centered and scaled to unit variance) faulty data. The contributions to the T^2 index have lower correct classification rates than those to the SPE index. Be aware that the dashed line does not change between Figs. 1(a) and 1(c) since isolation based on the data is independent of the monitoring statistic used. From the results for the SPE statistic, it is clear that the PD and RB contributions outperform data-based isolation at low fault magnitudes. The RB contributions achieve the highest isolation performance. For larger magnitudes the PD, RB and data-based correct isolation rates reach 100% which is in accordance with the theoretical guarantee of correct isolation for large single sensor faults. On the other hand, correct isolation using CD contributions is not guaranteed and the CD computation method is outperformed by PD and RB.

The correct isolation rates of CD, PD and RB contributions to the SPE and T^2 statistics for multiple sensor faults are plotted in Figs. 1(b) and 1(d), respectively. For multiple sensor faults, data-based isolation (dashed line) has overall higher correct isolation rates. PD contributions achieve the highest performance of the three contribution methods, because they are the most related to the data due to the multiplication of each linear combination with the variables' value in Eqs. 28 and 29. CD contributions on the other hand, exhibit the lowest isolation performance. For contributions to the SPE statistic, the CD contributions do not exceed 7% correct isolation rate due to the smearing effect. The RB contributions now take third place, despite having the highest performance for single sensor faults using the SPE index.

The influence of the selected number of principal components r is depicted in Fig. 2 for single sensor faults isolated with RB contributions to the SPE statistic (Fig. 2(a)) and multiple sensor faults isolated with PD contributions to the T^2 statistic (Fig. 2(b)). It is evident from the process model (Eq. 35) that the correct choice of the number of components is 3 since the generated data is governed by 3 latent variables (i.e., t_1, t_2 and t_3). Figs. 2(a) and 2(b) compare the correct isolation rate for the models with 2 (undermodeling), 3

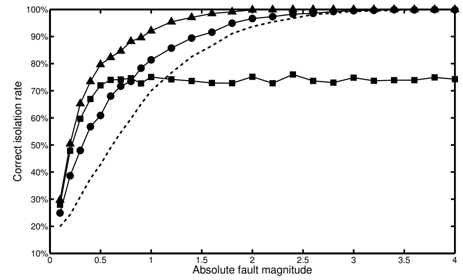

(a) Single sensor fault, SPE

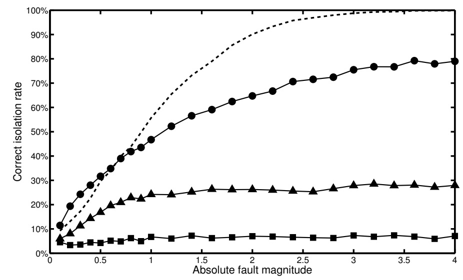

(b) Multiple sensor fault, SPE

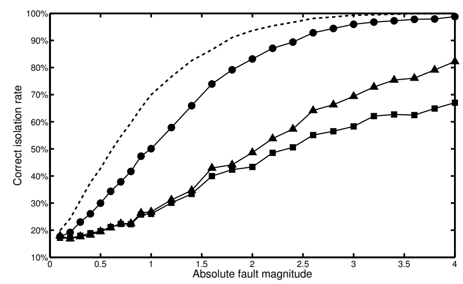

(c) Single sensor fault, T^2

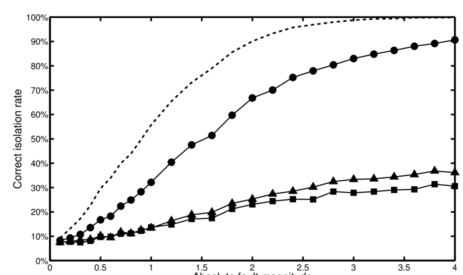

(d) Multiple sensor fault, T^2

Fig. 1. Correct isolation rates of CD (■), PD (•) and RB contributions (▲) to the SPE for (a) single and (b) multiple faults and to the T^2 for (c) single and (d) multiple faults. The dashed line depicts the correct classification rate achieved by using the absolute value of the mean centered and scaled (to unit variance) data.

(correct) and 4 (overmodeling) components. In Fig. 2(a), r-values different from 3 exhibit a lower correct isolation rate. In Fig. 2(b), the correct isolation rates if r equals 2 or 3 are comparable. For r equal to 4, the performance is significantly lower. Figs. 2(a) and 2(b) are representative for other combinations of fault type, statistic and contribution

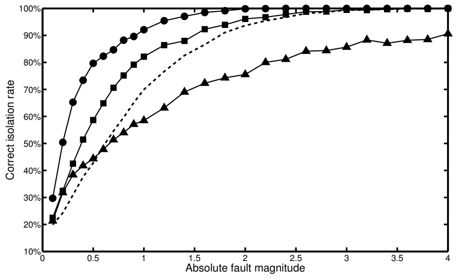

(a)

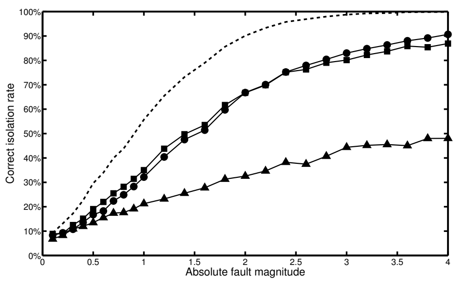

(b)

Fig. 2. Correct isolation rates of (a) single sensor faults with RB contributions to the SPE and (b) multiple sensor faults with PD contributions to the T^2 for 2 (■), 3 (•), and 4 (▲) principal components. The dashed line depicts the correct isolation rate achieved by using the absolute value of the mean centered and scaled (to unit variance) data.

computation method. These plots show that under- or over-modeling can have a negative effect on contribution fault isolation performance. Note that the correct isolation rate based on the absolute value of the data (dashed line) is independent of r and identical to Fig. 1.

V. Conclusions

Fault isolation confines the origin of a detected fault to a subset of the measured variables and in this way greatly narrows the search for the underlying cause. However, fault isolation is only a starting point: operators and plant engineers still need to bridge the gap between the fault isolation results and true fault diagnosis. Fault isolation techniques should aim to minimize this gap. Because PCA based techniques only model correlation, not causation, contribution plots highlight groups of correlated variables, which is the essence of contribution smearing.

The previous analysis (Section III) shows that to eliminate the smearing effect, the coefficients $\gamma_{i,j}$, $\delta_{i,j}$ and $\zeta_{i,j}$ in Eqs. 18, 19, 28, 29, 31 and 32 have to be set to zero, i.e., multivariate detection followed by univariate fault isolation. Hence, univariate isolation is superior to contribution plots when smearing presents a problem for fault isolation.

If a physical interpretation of the principal components is available, it is advisable to base the fault isolation on the deviation of the current scores $\mathbf{t}$ from those obtained under normal operating conditions. Isolating a detected disturbance to one or more scores allows one to link the detected disturbance with the underlying process dynamics captured by the principal components corresponding to these scores. In this case, the result of the fault isolation step is a group of variables corresponding to the faulty dynamics, rather than individual variables. Knowing what process dynamics are faulty provides operators with a good starting point to bridge the gap to true fault diagnosis based on their experience.

Unfortunately, a clear physical interpretation of each score is seldom available for process data. Section III demonstrated that the linear combination present at the core of each contribution computation method evidences the presence of smearing. The coefficients of this linear combination depend heavily on the principal components. If the interpretation of the principal components is unclear, using this information for fault isolation may confuse operators and increase the gap between isolation and diagnosis. The case study results (Section IV) have shown that the information contained in the principal components might be helpful for example when isolating single sensor faults with the RB technique, but might obscure the faulty variables for faults as relatively simple as multiple sensor faults where data based isolation achieves much higher correct isolation rates. Therefore, if no clear interpretation of the principal components is available, the authors advise to discard this information and perform multivariate detection followed by univariate fault isolation, i.e., basing fault isolation of general process faults on the deviation of the current measurements from their NOC values instead of contributions or scores.

References

[1] J. Westerhuis, S. Gurden, and A. Smilde, "Generalized contribution plots in multivariate statistical process monitoring," *Chemometr. Intell. Lab.*, vol. 51, pp. 95–114, 2000.
[2] I. Jollife, *Principal Component Analysis*. Springer Verlag, 1986.
[3] P. Geladi and B. Kowalski, "Partial Least-Squares Regression: a tutorial," *Anal. Chim. Acta*, vol. 185, pp. 1–17, 1986.
[4] J. Kresta, J. MacGregor, and T. Marlin, "Multivariate statistical monitoring of processes," *Can. J. Chem. Eng.*, vol. 69, no. 1, pp. 35–47, 1991.
[5] P. Nomikos and J. MacGregor, "Multi-way partial least squares in monitoring batch processes," *Chemometr. Intell. Lab.*, vol. 30, pp. 97–108, 1995.
[6] P. Miller, R. Swanson, and C. Heckler, "Contribution plots: a missing link in multivariate quality control," *Appl. Math. Comp. Sci.*, vol. 8, pp. 775–792, 1998.
[7] A. Tates, D. Louwerse, A. Smilde, G. Koot, and H. Berndt, "Monitoring a PVC batch process with multivariate statistical process control charts," *Ind. Eng. Chem. Res.*, vol. 38, pp. 4769–4776, 1999.
[8] M. Weighell, E. Martin, and A. Morris, "The statistical monitoring of a complex manufacturing process," *J. Appl. Stat.*, vol. 28, no. 3-4, pp. 409–425, 2001.
[9] S. Bezergianni and A. Kalogianni, "Application of principal component analysis for monitoring and disturbance detection of a hydrotreating process," *Ind. Eng. Chem. Res.*, vol. 47, pp. 6972–6982, 2008.
[10] R. Berber, I. Atasoy, M. Yuceer, and G. Deniz, "On-line statistical process monitoring and fault diagnosis in batch bakers yeast fermentation," *Chem. Eng. Technol.*, vol. 32, no. 4, pp. 650–658, 2009.
[11] C. Alcala and S. Qin, "Reconstruction-based contribution for process monitoring," *Automatica*, vol. 45, pp. 1593–1600, 2009.
[12] J. MacGregor, C. Jaeckle, C. Kiparissides, and M. Koutoudi, "Process monitoring and diagnosis by multiblock PLS methods," *AIChE J.*, vol. 40, no. 5, pp. 826–838, 1994.
[13] J. MacGregor and T. Kourti, "Statistical process control of multivariate processes," *Control Eng. Pract.*, vol. 3, no. 3, pp. 403–414, 1995.
[14] C. Alcala and S. Qin, "Analysis and generalization of fault diagnosis methods for process monitoring," *J. Process Contr.*, vol. 21, pp. 322–330, 2011.